Arabian Journal of Chemistry (2015) xxx, xxx–xxx

King Saud University

Arabian Journal of Chemistry

www.ksu.edu.sa
www.sciencedirect.com

ORIGINAL ARTICLE

Inhibition effect of butan-1-ol on the corrosion behavior of austenitic stainless steel (Type 304) in dilute sulfuric acid

R.T. Loto [a,b,*], C.A. Loto [a,b], A.P.I. Popoola [b], T. Fedotova [b]

[a] Department of Mechanical Engineering, Covenant University, Ota, Ogun State, Nigeria
[b] Department of Chemical, Metallurgical & Materials Engineering, Tshwane University of Technology, Pretoria, South Africa

Received 1 October 2014; accepted 14 December 2014

KEYWORDS

Corrosion;
Adsorption;
Steel;
Butan-1-ol

Abstract The electrochemical behavior of austenitic stainless steel (Type 304) in 3 M sulfuric acid with 3.5% recrystallized sodium chloride at specific concentrations of butan-1-ol was investigated with the aid of potentiodynamic polarization, open circuit measurement and weight loss technique. Butan-1-ol effectively inhibited the steel corrosion with a maximum inhibition efficiency of 78.7% from weight-loss analysis and 80.9% from potentiodynamic polarization test at highest concentration studied. Adsorption of the compound obeyed the Freundlich isotherm. Thermodynamic calculations reveal physiochemical interactions and spontaneous adsorption mechanism. Surface characterizations showed the absence of corrosion products and topographic modifications of the steel. Statistical analysis depicts the overwhelming influence and statistical significance of inhibitor concentration on the inhibition performance.

1. Introduction

Austenitic steels are non-magnetic stainless steels that contain high levels of chromium and nickel, and low levels of carbon. Known for their formability and resistance to corrosion, austenitic steels are the most widely used grade of stainless steel. They have good formability and weldability, as well as excellent toughness, particularly at low, or cryogenic, temperatures. Austenitic steel also has a low yield stress and relatively high tensile strength (Terence, 2014). The non-magnetic properties combined with exceptionally high toughness at all temperatures make these steels an excellent selection for a wide variety of applications. The annual world production of the steel is approximately 400 million, and of this about 2% is stainless. Demand for stainless steels increases by 3–5% per annum with major applications in extractive industries, petrochemicals, chemical processing plants, automotive and aerospace structural alloy, construction materials petroleum industry, marine environments and sugar industries, food industry and breweries, energy production, pulp and paper and textile industry (Béla, 2014).

* Corresponding author at: Department of Mechanical Engineering, Covenant University, Ota, Ogun State, Nigeria. Tel.: +234 8084283392.
E-mail address: tolu.loto@gmail.com (R.T. Loto).
Peer review under responsibility of King Saud University.

Production and hosting by Elsevier

http://dx.doi.org/10.1016/j.arabjc.2014.12.024

Please cite this article in press as: Loto, R.T. et al., Inhibition effect of butan-1-ol on the corrosion behavior of austenitic stainless steel (Type 304) in dilute sulfuric acid. Arabian Journal of Chemistry (2015), http://dx.doi.org/10.1016/j.arabjc.2014.12.024

The stainless steels contain sufficient chromium to form a passive film of chromium oxide, which prevents further surface corrosion by blocking oxygen diffusion to the steel surface and blocks corrosion from spreading into the metal's internal structure, and due to the similar size of the steel and oxide ions they bond very strongly and remain attached to the surface (Jianhai, 2014). Under certain conditions, particularly involving high concentrations of chlorides, reducing acids, in some types of combustion where the atmosphere is reducing and under the combined effects of stress they do in fact suffer from certain types of corrosion resulting in rapid deterioration of the alloy due to the breakdown of the passive film.

The most effective and economical measure of corrosion control is through the use of inhibitors with particular attention on organic compounds. A significant number of compounds evaluated displays good anticorrosive characteristics; however most of them are highly toxic to both man and the environment (Neha et al., 2013). These toxic effects and environmental damage connected with the passage of such chemicals have resulted in the research and development of organic compounds for corrosion inhibition. Organic compounds have shown good application as corrosion inhibitors for steel in acidic environments (Giacomelli et al., 2004; Satapathy et al., 2009; Mathiyarasu et al., 2001; Ochao et al., 2004; Oguzie, 2004; Shalaby and Osman, 2001; Ebenso, 2003). Such compounds typically contain nitrogen, oxygen or sulfur in a conjugated system, and function via adsorption of the molecules on the metal surface, creating an impenetrable barrier to corrosive attack (Quraishi and Sharma, 2002). This investigation aims to assess the inhibitive effect of butan-1-ol (BTU) on the electrochemical corrosion behavior of Type 304 austenitic stainless steel in dilute sulfuric acid chloride. BTU is a primary alcohol with a 4-carbon structure and the molecular formula of C_4H_9OH, belonging to the higher and branched-chain alcohols without any record of harm to humans and the environment (see Fig. 1).

2. Materials and methods

2.1. Material

Commercially available Type 304 austenitic stainless steel was used for all experiments of average nominal composition; 18.11% Cr, 8.32% Ni and 68.32% Fe. The material is cylindrical with a diameter of 18 mm.

2.2. Inhibitor

Butan-1-ol (BTU) a brownish, translucent liquid is the inhibitor used. The structural formula of BTU is shown in Fig. 2. The molecular formula is C_4H_9OH while the molar mass is 74.122 g/mol.

BTU was prepared in volumetric concentrations of 2.5%, 5%, 7.5%, 10%, 12.5% and 15% per 200 ml of the acid solution respectively.

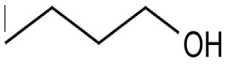

Figure 1 Chemical structure of butan-1-ol (BTU).

2.3. Test media

3 M sulfuric acid with 3.5% re-crystallized sodium chloride of Analar grade was used as the corrosion test media.

2.4. Preparation of test specimens

The cylindrical stainless steel (18 mm dia.) was mechanically cut into a number of test specimens of dimensions in length ranging from 17.8 mm and 18.8 mm coupons. The two surface ends of each of the specimen were ground with silicon carbide abrasive papers of 80, 120, 220, 800 and 1000 grits. They were then polished with 6.0 μm to 1.0 μm diamond paste, washed with distilled water, rinsed with acetone, dried and stored in a dessicator for further weight-loss test and linear polarization.

2.5. Weight-loss experiments

Weighted test species were fully and separately immersed in 200 ml of the test media at specific concentrations of BTU for 360 h at ambient temperature of 25 °C. Each of the test specimens was taken out every 72 h, washed with distilled water, rinsed with acetone, dried and re-weighed. Plots of weight-loss (mg) and corrosion rate (mm/y) versus exposure time (h) (Figs. 2 and 3) for the two test media and those of percentage inhibition efficiency ($\%IE$) (calculated) versus exposure time (h) and percentage BTU concentration (Figs. 4 and 5) were made from Table 1.

The corrosion rate (R) calculation is from Eq. (1):

$$R = \left[\frac{87.6W}{\mathrm{DAT}}\right] \tag{1}$$

where W is the weight loss in milligrams, D is the density in g/cm^2, A is the area in cm^2, and T is the time of exposure in hours. The $\%IE$ was calculated from the relationship in Eq. (2).

$$\%IE = \left[\frac{W_1 - W_2}{W_1}\right] \times 100 \tag{2}$$

W_1 and W_2 are the weight loss (in the absence and presence of BTU). The $\%IE$ was calculated for all the inhibitors every 72 h during the course of the experiment, while the surface coverage is calculated from the relationship:

$$\theta = \left[1 - \frac{W_2}{W_1}\right] \tag{3}$$

where θ is the substance amount of adsorbate adsorbed per gram (or kg) of the adsorbent. W_1 and W_2 are the weight loss of austenitic stainless steel coupon in free and inhibited acid chloride solutions respectively.

2.6. Open circuit potential measurements

A two-electrode electrochemical cell with a silver/silver chloride was used as reference electrode. The measurements of OCP were obtained with Autolab PGSTAT 30 ECO CHIMIE potentiostat. Resin mounted test electrodes/specimens with an exposed surface of 254 mm^2 were fully and separately immersed in 200 ml of the test media (acid chloride) at specific concentrations of BTU for a total of 288 h. The potential of

Please cite this article in press as: Loto, R.T. et al., Inhibition effect of butan-1-ol on the corrosion behavior of austenitic stainless steel (Type 304) in dilute sulfuric acid. Arabian Journal of Chemistry (2015), http://dx.doi.org/10.1016/j.arabjc.2014.12.024

each of the test electrodes was measured every 48 h. Plots of potential E (mV) versus immersion time T (h) (Fig. 6) for the test medium were made from the tabulated values in Table 2.

2.7. Linear polarization resistance

Linear polarization measurements were carried out using, a cylindrical coupon embedded in resin plastic mounts with exposed surface of 254 mm^2. The electrode was polished with different grades of silicon carbide paper, polished to 6 μm, rinsed by distilled water and dried with acetone. The studies were performed at ambient temperature of 25 °C with Autolab PGSTAT 30 ECO CHIMIE potentiostat and electrode cell containing 200 ml of electrolyte, with and without inhibitor. A graphite rod was used as the auxiliary electrode and silver chloride electrode (SCE) was used as the reference electrode. The steady state open circuit potential (OCP) was noted. The potentiodynamic studies were then made from −1.5 V versus OCP to +1.5 V versus OCP at a scan rate of 0.00166 V/s and the corrosion currents were registered. The corrosion current density (j_{corr}) and corrosion potential (E_{corr}) were determined from the Tafel plots of potential versus log I. The corrosion rate (R), the degree of surface coverage (θ) and the percentage inhibition efficiency (%IE) were calculated as follows.

$$R = \frac{0.00327^{\times} i_{corr}^{\times} eq.wt}{D} \quad (4)$$

where i_{corr} is the current density in μA/cm^2, D is the density in g/cm^3; $eq.wt$ is the specimen equivalent weight in grams.

The percentage inhibition efficiency (%IE) was calculated from corrosion current density values using the equation.

$$\%IE = 1 - \left[\frac{R_2}{R_1}\right] \times 100 \quad (5)$$

where R_1 and R_2 are the corrosion rates in absence and presence of inhibitors, respectively.

2.8. Scanning electron microscopy characterization

The surface morphology of the uninhibited and inhibited stainless steel specimens was investigated after weight-loss analysis in 3 M H_2SO_4 solution using Jeol scanning electron microscope for which SEM micrographs were obtained (Fig. 9).

2.9. X-ray diffraction analysis

X-ray diffraction (XRD) patterns of the film formed on the metal surface with and without DMAE addition were analyzed using a Bruker AXS D2 phaser desktop powder diffractometer with monochromatic Cu Kα radiation produced at 30 kV and 10 mA, with a step size of 0.03° 2θ. The Measurement program is the general scan xcelerator.

2.10. Statistical analysis

Two-factor single level experimental ANOVA test (F-test) was used to analyze the separate and combined effects of the percentage concentrations of BTU and exposure time on the inhibition efficiency of BTU in the corrosion of inhibition of austenitic stainless steels in 3 M H_2SO_4 solution and to investigate the statistical significance of the effects. The F-test was used to examine the amount of variation within each of the samples relative to the amount of variation between the samples.

The Sum of squares among columns (exposure time) was obtained with the Eq. (6).

$$SS_c = \frac{\sum T_c^2}{nr} - \frac{T^2}{N} \quad (6)$$

Sum of Squares among rows (inhibitor concentration)

$$SS_r = \frac{\sum T_r^2}{nc} - \frac{T^2}{N} \quad (7)$$

Total Sum of Squares

$$SS_{Total} = \sum x^2 - \frac{T^2}{N} \quad (8)$$

3. Results and discussion

3.1. Weight-loss measurements

Weight-loss of austenitic stainless steel at various time intervals, in the absence and presence of BTU concentrations in 3 M H_2SO_4 was studied. The values of weight-loss (W), corrosion rate (R) and the percentage inhibition efficiency (%IE) are presented in Table 1. Figs. 2–4 show the variation of weight-loss, corrosion rate and percentage inhibition efficiency versus exposure time at specific BTU concentrations while Fig. 5

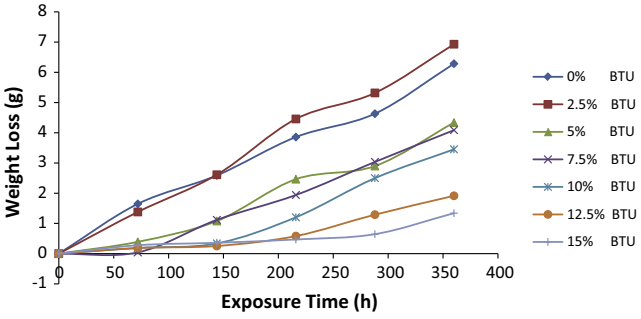

Figure 2 Variation of weight-loss with exposure time for samples (A–G) in 3 M H_2SO_4.

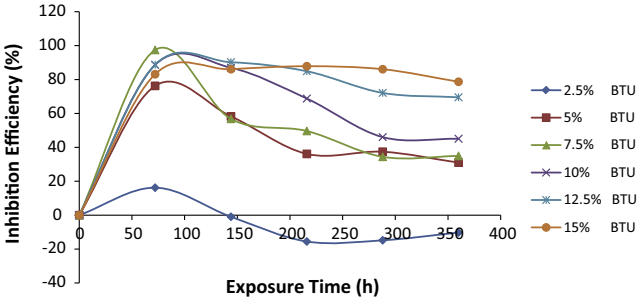

Figure 3 Plot of inhibition efficiencies of sample (A–G) in 3 M H_2SO_4 during the exposure period.

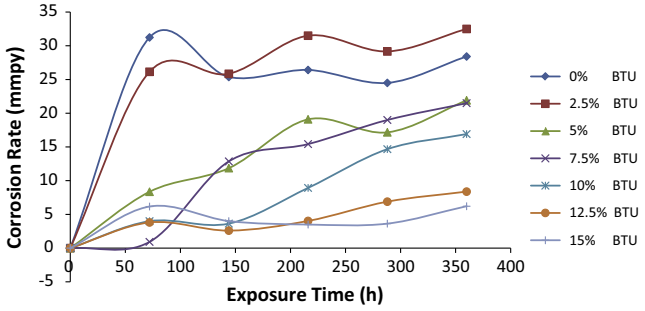

Figure 4 Effect of percentage concentration of BTU on the corrosion rate of austenitic stainless steel in 3 M H_2SO_4.

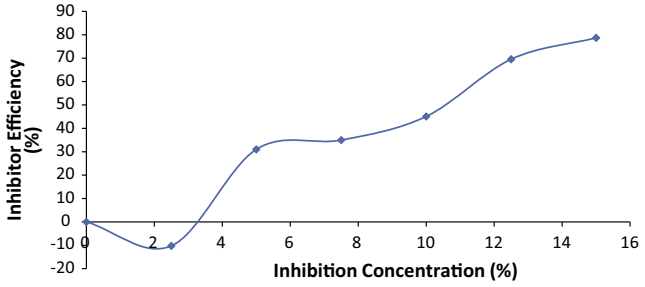

Figure 5 Variation of percentage inhibition efficiency of BTU with inhibitor concentration in 3 M H_2SO_4.

shows the variation of %*IE* with inhibitor concentration. The curves show increase in %*IE* with increase in BTU concentration accompanied by a significant decrease in corrosion rate. As BTU concentration increases the barrier film formed on the steel surface becomes more compact, effectively separating the surface from aggressive anionic species within the test solution while at the same time stifling the redox reactions associated with the corrosion process. The diffusion of Fe^{2+} and Cl^-/SO_4^{2-} is thus effectively inhibited.

The barrier film is strongly adsorbed through physisorption mechanisms by weak van der waals forces. There is no evidence of it been chemically bonded onto the surface of the steel. Effective inhibition occurred from 12.5% to 15% BTU most probably through the adsorption of the functional hydroxyl group of the inhibitor on the stainless steel surface by the interaction of π-electrons or lone pair electron of hetero atoms with the metal.

3.2. Open circuit potential measurement

The open-circuit potential value of the specimen electrodes was studied for a total of 288 h in the acid chloride solutions as shown in Table 2. Fig. 6 shows the variation of open-circuit potentials with time of BTU in 3 M H_2SO_4 chloride solutions. The corrosion potentials values of 0% and 2.5% BTU concentrations reveal severe active throughout the exposure period. The corrosion potentials values between 5% and 15% BTU concentration showed a sharp variation from 0% to 2.5% BTU due to the instantaneous action of BTU in aiding the passivation of the stainless steel in the corrosive medium. This passivation was not sustained through the exposure period as observed from the potential values for 5% to 10% BTU concentration. There was a transition within the first 48 h to transpassivity and corrosion failure which continued to the end of the immersion period. The above observation is further supported from the low inhibition efficiency (Table 2) obtained at these BTU concentrations (5–10% BTU). The potential values for 12.5–15% BTU concentration remained within the passive corrosion potentials for the whole exposure period, an indication of the effectiveness of BTU at these concentrations as shown from the inhibition efficiency.

Analysis of the potential values reveals the nature of the intermolecular bond between the inhibitor molecules and the steel sample. From 2.5% to 10% BTU concentration, there was severe active corrosion to mild corrosion due to the inability of BTU to form an impenetrable barrier between the steel surface and the reactive anions responsible for corrosion. But there is a progressive but slow improvement of the inhibition efficiency which remained at values below 50%.

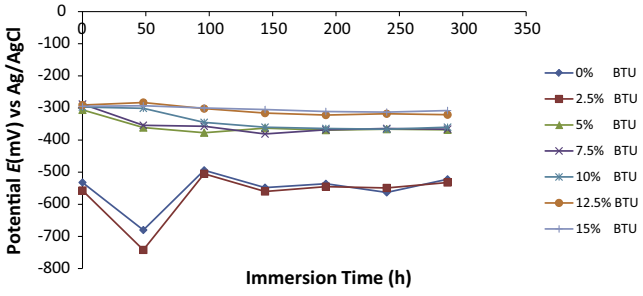

Figure 6 Variation of potential with immersion time for potential measurements in 3 M H_2SO_4.

Table 1 Data obtained from weight loss measurements for austenitic stainless steel in 3 M H_2SO_4 in presence of specific concentrations of the BTU at 360 h.

Sample	Inhibitor concentration (%)	Inhibitor concentration (molarity)	Weight loss (mg)	Corrosion rate (mm/y)	Inhibition efficiency (%)
A	0	0	6.286	28.4	0
B	2.5	0.00034	6.930	32.5	−10.3
C	5	0.00068	4.337	21.9	31
D	7.5	0.00101	4.088	21.5	35
E	10	0.00135	3.453	16.9	45.1
F	12.5	0.00169	1.915	8.40	69.5
G	15	0.00202	1.340	6.20	78.7

Please cite this article in press as: Loto, R.T. et al., Inhibition effect of butan-1-ol on the corrosion behavior of austenitic stainless steel (Type 304) in dilute sulfuric acid. Arabian Journal of Chemistry (2015), http://dx.doi.org/10.1016/j.arabjc.2014.12.024

Table 2 Data obtained from potential measurements for austenitic stainless steel in 3 M H_2SO_4 in presence of specific concentrations of the BTU.

BTU concentration (%) Exposure time (h)	0	2.5	5	7.5	10	12.5	15
0	−532	−557	−306	−288	−297	−291	−295
48	−680	−742	−361	−354	−301	−283	−293
96	−494	−505	−377	−357	−345	−302	−300
144	−548	−560	−363	−381	−360	−316	−305
192	−536	−545	−369	−368	−364	−322	−311
240	−563	−549	−366	−364	−366	−318	−313
288	−522	−532	−368	−366	−360	−321	−308

The intermolecular force no doubt would not have involved charge transfer or electron sharing responsible for chemisorption, instead from the potential values the force most prevalent is the weak van der waals force.

Beyond 10% BTU concentration the corrosion potential values is well within passivity as earlier mentioned due to the availability of the more BTU molecules to minimize the redox reactions responsible for corrosion, though there is greater tendency for inhibition of hydrogen evolution and oxygen reduction reactions. At these higher concentrations there is a tendency for physiochemical reaction due to the presence of heteroatom i.e. oxygen, responsible for nucleophilic reactions within the corrosive medium. Increase in the number of oxygen atoms available for charge sharing results in greater corrosion inhibition.

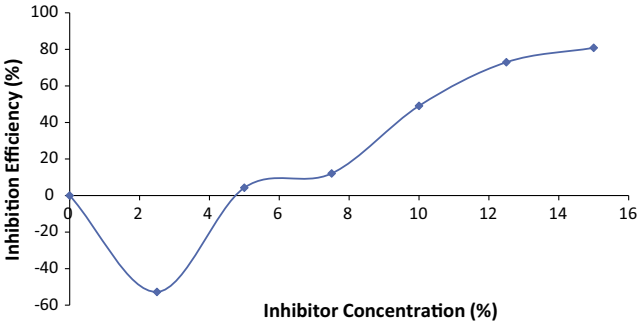

Figure 8 Relationship between %*IE* and inhibitor concentration for polarization test in 3 M H_2SO_4.

3.3. Polarization studies

Potentiostatic potential was cursorily examined from −1.50 to +1.50 V versus SCE at a scan rate of 0.00166 mV s^{-1}. This allows for electrodynamic equilibrium measurement. The effect of the addition of BTU on the anodic and cathodic polarization curves of austenitic stainless steel (Type 304) in 3 M H_2SO_4 at 25 °C was studied at ambient temperature of 25 °C. Fig. 7 shows the polarization curves of the stainless steel in absence and presence of BTU at specific concentrations in 3 M H_2SO_4. The effectiveness of BTU depends on the value of its concentrations as shown in Figs. 8. The corrosion rate reduced drastically at 12–15% concentration. As observed in above figure a progressive increase in BTU concentration up to these values results in the availability of more BTU molecules to significantly form an impenetrable compact protective barrier on the alloy surface thus preventing anodic oxidation.

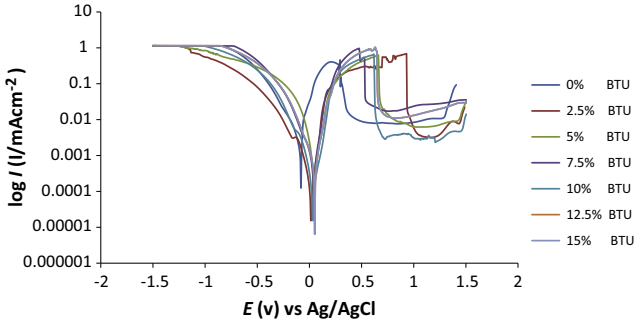

Figure 7 Comparison plot of cathodic and anodic polarization scans for austenitic stainless steel in 3 M H_2SO_4 + 3.5% NaCl solution in the absence and presence of specific concentrations of BTU.

Results obtained using linear polarization resistance method show that BTU significantly influenced the electrochemical process of corrosion. Generally, all scans in Fig. 7 exhibited slightly similar cathodic behavior over the potential domain examined, but the anodic behavior is virtually the same indicating similar redox reactions irrespective of BTU concentration.

The cathodic and anodic Tafel constants without BTU differ from the values obtained for BTU concentration, these values remained generally the same before a sharp change at 12.5–15% BTU to lower values which coincide with the low corrosion rate and high inhibition efficiency; this further proves the similar redox reaction which occurred during the electrolytic process. The redox reactions at 12.5–15% slow down in response to the protective film on the steel surface which blocks the reactive sites on the metal and inhibits hydrogen evolution reactions. The corrosion potential in Fig. 7 shifts toward and varies within positive potentials as BTU concentration increases, an indication of the affinity of the organic compound for anodic reaction. This will be discussed further in detail.

Electrochemical variables such as, corrosion potential (E_{corr}), corrosion current (i_{corr}), corrosion current density (I_{corr}), cathodic Tafel constant (bc), anodic Tafel slope (ba), surface coverage (θ) and percentage inhibition efficiency (%*IE*) were calculated and given in Table 3. The corrosion current density (I_{corr}) and corrosion potential (E_{corr}) were determined by the intersection of the extrapolating anodic and cathodic Tafel lines, %*IE* was calculated from Eq. (9).

Table 3 Data obtained from polarization resistance measurements for austenitic stainless steel in 3 M H_2SO_4 in presence of DMAE.

Inhibitor concentration (%)	Corrosion rate (mm/yr)	%*IE*	R_p (Ω)	E_{corr}, obs (V)	E_{corr}, cal (V)	i_{corr} (A)	I_{corr} (A/cm^2)	*bc* (V/dec)	*ba* (V/dec)
0	5.35	0	6.58	−0.355	−0.036	1.19E−03	4.69E−04	0.043	0.031
2.5	8.18	−52.8	1.42	0.355	0.028	1.82E−03	7.17E−04	0.011	0.013
5	5.12	4.3	3.99	0.329	0.042	1.14E−03	4.49E−04	0.018	0.025
7.5	4.72	12.1	4.29	0.422	0.042	1.05E−03	4.13E−04	0.051	0.013
10	2.71	49.1	21.49	0.369	0.033	6.04E−04	2.38E−04	0.079	0.048
12.5	1.45	73	49.91	0.355	0.051	3.23E−04	1.27E−04	0.163	0.048
15	1.02	80.9	54.08	0.417	0.051	2.28E−04	8.98E−05	0.061	0.053

$$\%IE = \frac{\boldsymbol{R}_1 - \boldsymbol{R}_2}{\boldsymbol{R}_1}\% \quad (9)$$

BTU appeared to act as a mixed type inhibitor due to its influence on the cathodic and anodic reactions in the corrosive medium, with the anodic effect being more significantly suppressed than the cathodic reactions based on observation of the displacement in E_{corr} values (Li et al., 2008). The concentration of butan-1-ol at 2.5% is not sufficient to adsorb or bond onto the metal surface or raise the over potential for hydrogen ion to produce any significant inhibiting effect, but instead it accelerates the corrosion process resulting in increased weight loss of the steel (Sastri, 2012; Maan et al., 2012; Winston and Papavinasam, 2000; Hans, 2005). The presence of the hydroxyl functional group in the compound increased its solubility thus enabling it to be easily bonded unto the alloy electrode, however the anodic reaction of metal dissolution could not be suppressed effectively before 12.5% BTU concentration for the steel electrode due to rapid desorption of inhibitor. The inhibitor adsorbed onto the metal surface and impedes the passage of metal ions from the oxide-free metal surface into the solution, by merely blocking the reaction sites of the metal surface thus affecting the anodic reaction mechanism (Rudresh and Mayanna, 1977). The anodic Tafel slope values can be attributed to diffusion control, where the inhibitor molecules are adsorbed via their hydroxyl functional group through the heterocyclic oxygen atoms on to the steel surface forming a protective layer through physical attraction (Chen and Zhao, 2012; Tsygankova et al., 2014; Amitha Rani and Bharathi Bai, 2011).

3.4. Mechanism of inhibition by BTU

The functional group of butan-1-ol is the hydroxyl group (OH^-) (Abbasov et al., 2013). The hydroxyl groups in this compound are polarized in the acid solution so that the oxygen atom becomes an electron donor. The hydroxyl group is responsible for electrostatic attraction with the metal (Dieter, 2007; Physisorption, 2014). In the presence of BTU, corrosion is inhibited by adsorption of the BTU molecules on the metal surface. Protection by BTU is generally enhanced by the electrophilic interaction of iron ions in the electrolytic reactions responsible for the formation of surface films. Adsorption of protonated BTU molecule on the metal surface takes place through the *pi*-electron of oxygen atoms (Shylesha et al., 2012; Obi-Egbedi and Obot, 2013).

Inhibition mechanism of BTU molecules can also be explained from another angle. The oxygen atoms are attracted to the negatively charged metal surface created by the adsorbed chloride ion (Xiumei et al., 2012). The low energy vacant d-orbital of iron and molecules of BTU having relatively loosely bound electrons from the hetero-atoms is responsible for this interaction (Xiumei et al., 2013). Under this electrochemical condition the lone pairs on the oxygen atom of make them Lewis Bases while the metal acts as an electrophile, their interaction results in bond formation over the entire metal surface. In the form of neutral molecules BTU may be adsorbed on the metal surface involving the displacement of water molecules from the metal surface and sharing of electrons between the oxygen atom and the iron surface.

3.5. Scanning electron microscopy analysis

The SEM images of the stainless steel surfaces before immersion in the acidic media; in 3 M H_2SO_4 solution after 360 h of immersion with and without BUT inhibitor are shown in Fig. 9(a–d), respectively. Fig. 9a and b shows the steel sample before immersion, the lined surface is due to cutting during preparation. Fig. 9c shows the steel surfaces after 360 h of exposure in 3 M H_2SO_4 without BTU, while Fig. 9d shows the steel surface in the acid media with BTU. In the absence of BTU, a very rough and porous surface is observed in Fig. 9c; large number of pits, micro pits and badly corroded topography of the stainless steel coupons are visible as a result of the corrosive actions of chloride and sulfate ions due to the breakdown of the passive film of chromium oxide. The high diffusion of the aggressive anions through cracks and passive film occurs faster than the rate of repassivation of the steel.

The competitive diffusion of chlorides and sulfates into the oxide/liquid interface of the steel surface displaces the adsorbed oxygen species and chromium cations responsible for passivation. This causes the diffusion of Fe^{2+} into the solution. This result is the rapid formation of voids which develop and grow at specific sites such as regions of defects and flaws, inclusions and sites susceptible to pitting in general. Addition of BTU to the acid solution causes the formation of a protective film over the steel capable of inhibiting steel corrosion effectively at high concentrations. Fig. 9d shows the stainless steel in 15% BTU concentration after exposure. The slight uneven topography as compared to Fig. 9c is due to the delayed action of BTU due to its inability to chemisorb on the steel specimen during exposure. The forces of attraction between BTU and the stainless steel are weak van der waals forces calculated from Gibbs free energy of adsorption and the values of equilibrium constant of adsorption. The forces

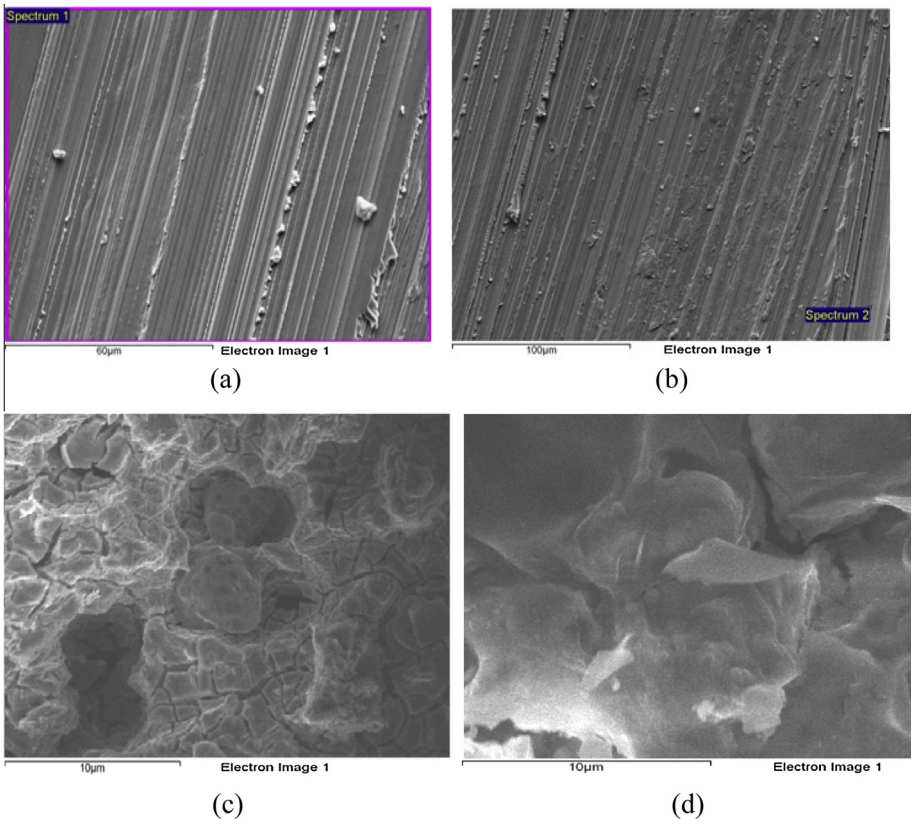

Figure 9 SEM micrographs of: (a) Austenitic stainless steel, (b) Austenitic stainless steel, (c) Austenitic stainless steel in 3 M H_2SO_4, (d) Austenitic stainless steel in 3 M H_2SO_4 with BTU.

results in physical attraction (physisorption) through its hydroxyl functional groups, thus the ability of BTU to inhibit corrosion is limited and effective only at high concentrations.

The adsorption of the negatively charged chloride and sulfate anions on the stainless steel surface creates an excess negative charge leading to cations (protonated BTU) adsorption on the steel surface through electrostatic attraction. The protonated BTU molecules adsorbs on the stainless steel surface weakly via chloride ions which form an interconnecting bridge between positively charged stainless steel surface and protonated BTU. The presence of BTU in the solution, causes a sharp difference in morphology of the steel surface compared to Fig. 9c.

3.6. XRD analysis

X-ray diffraction (XRD) patterns of stainless steel surfaces from the acid test solutions are shown in Fig. 10(a and b) while Tables 4 and 5) show the phase compositions present. Fig. 10a (3 M H_2SO_4 without BTU) showed the peak values at $2\theta = 89.4°$ and 111.2° indicating the presence of iron oxides i.e. products of corrosion due to sample deterioration and breakdown. In Fig. 10b, the phases present are non-corrosion compounds i.e. impurities, inclusions etc that have no influence on the overall corrosion process. The absence of corrosion products is due to the inhibition action of BTU. BTU effectively aided the passivation of steel by electrostatic attraction (physisorption) and minimal chemical reaction resulting in slight

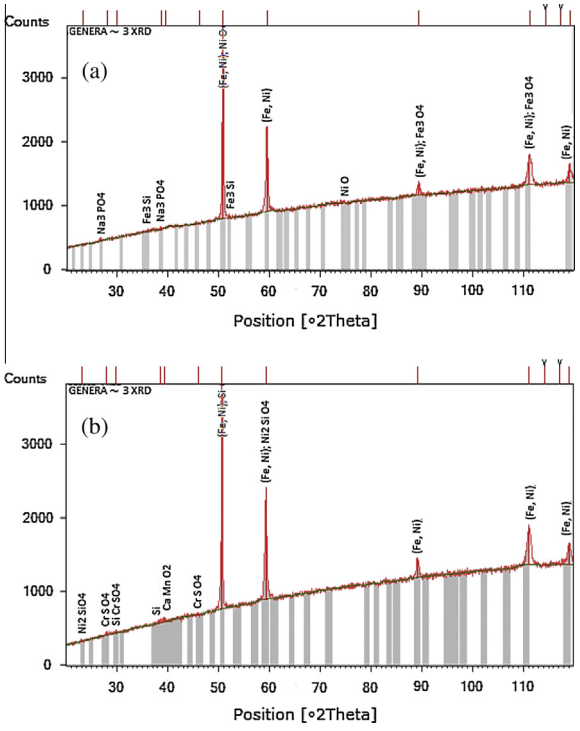

Figure 10 XRD pattern of the surface film formed on austenitic stainless steel after immersion in 3 M H_2SO_4 (a) without BTU (b) with BTU.

Table 4 Identified patterns list for XRD analysis of austenitic stainless steel in 3 M H_2SO_4 without BTU.

Ref. code	Score	Compound name	Displacement [°2Theta]	Scale factor	Chemical formula
00-047-1417	61	Taenite, syn	−0.095	0.974	(Fe, Ni)
00-065-3005	41	Iron silicon	−0.993	0.01	Fe_3Si
00-008-0087	38	Iron oxide	0.173	0.078	Fe_3O_4
01-084-0195	25	Sodium phosphate	−0.723	0.016	Na_3PO_4
01-089-5881	21	Nickel oxide	−0.018	0.341	NiO

Table 5 Identified patterns list for XRD analysis of austenitic stainless steel in 3 M H_2SO_4 with BTU.

Ref. code	Score	Compound name	Displacement [°2Theta]	Scale factor	Chemical formula
00-047-1417	58	Taenite, syn	−0.257	0.911	(Fe, Ni)
00-040-0932	0	Silicon	−0.343	0.313	Si
00-045-1266	30	Calcium manganese oxide	−0.368	0.021	$CaMnO_{2.98}$
00-021-0244	24	Chromium sulfate	0.303	0.007	$CrSO_4$
01-070-1852	0	Nickel silicate	0.928	0.024	Ni_2SiO_4

Table 6 Data obtained for the values of Gibbs free energy, surface coverage and equilibrium constant of adsorption at varying concentrations of BTU in 3 M H_2SO_4.

Inhibitor concentration (M)	Equilibrium constant of adsorption (K_{ads})	Free energy of adsorption (ΔG_{ads}) (kJ/mol)	Surface coverage (θ)
0	0	0	0
0.000337	−5367.97	0	−0.102
0.000675	6320.198	−31.63	0.3101
0.001012	4110.669	−30.57	0.3497
0.001349	3584.866	−30.23	0.4507
0.001687	4081.637	−30.55	0.6954
0.002024	3605.861	−30.24	0.7868

covalent bonding for effective corrosion inhibition (see Table 6).

3.7. Adsorption isotherm

The mechanism of corrosion inhibition can be explained on the basis of adsorption behavior of BTU on the metal surface through adsorption isotherms. The adsorptive behavior of a corrosion inhibitor provides in-depth assessment of the nature of the metal–inhibitor interaction (Quraishi et al., 2004; Hirozawa, 1995). Freundlich adsorption isotherm (Fig. 11) was applied to describe the adsorption mechanism for BTU compounds in 3 M H_2SO_4. Freundlich isotherm states that the relationship between the amount and concentration of BTU molecules absorbed onto the steel varies at different concentrations. The plot in Fig. 6 fitted the Freundlich isotherm, according to Eq. (10).

$$\theta = KC^n \tag{10}$$

$$\log\ \theta = n\log\ C + \log\ K \tag{11}$$

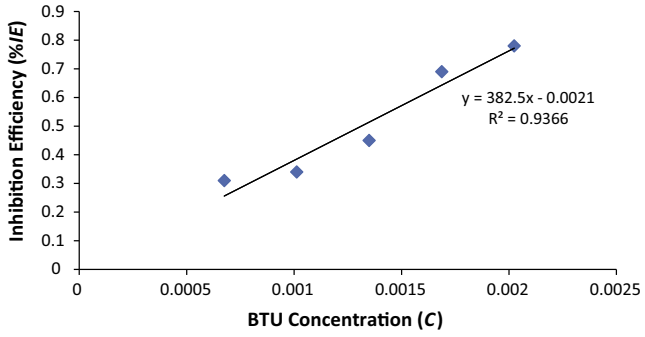

Figure 11 Plots of inhibition efficiency versus BTU concentration.

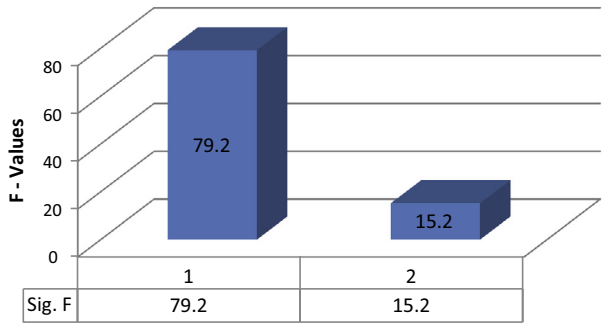

Figure 12 Influence of inhibitor concentration and exposure time on inhibition efficiency BTU in 3 M H_2SO_4.

Table 7 Analysis of variance (ANOVA) for inhibition efficiency of BTU inhibitor in 3 M H_2SO_4 (at 95% confidence level).

Source of variation	Sum of squares	Degree of freedom	Mean square	Mean square ratio	Min. MSR at 95% confidence	
					Significance F	F (%)
Inhibitor concentration	26743.52	5	5348.7	528.12	2.71	79.2
Exposure time	4725.24	4	1181.31	116.64	2.87	15.2
Residual	202.56	20	10.13			
Total	31671.32	29				

n is a constant depending on the characteristics of the adsorbed molecule, where $0 < n < 1$, K is the adsorption–desorption equilibrium constant denoting the strength of interaction in the adsorbed layer. Positive and large values of K obtained (Table 6) suggest significantly strong interaction between BTU molecule and the metal surface (Atkin, 1994; Unuabonah et al., 2007).

3.8. Thermodynamics of the corrosion process

The values of free energy change i.e. Gibbs free energy (ΔG_{ads}) for the adsorption process can be evaluated from the equilibrium constant of adsorption using the following equation.

$$\Delta G_{ads} = -2.303RT\log[55.5K_{ads}] \quad (12)$$

where 55.5 is the molar concentration of water in the solution, R is the universal gas constant, T is the absolute temperature and K_{ads} is the equilibrium constant of adsorption. K_{ads} is related to surface coverage (θ) by the following equation.

$$\theta = KC^n \quad (13)$$

$$n = 0.0023$$

The dependence of free energy of adsorption (ΔG_{ads}) of BTU on surface coverage is due to the heterogeneous nature of the steel electrode. On the steel there are variations because of surface inhomogeneities, flaws, cracks, defect, non-metallic inclusions, etc., thus the differential value of adsorption energies as observed in the experimental data (Table 6). Values of ΔG_{ads} around -20 kJ/mol or below depict physisorption mechanisms and those of about -40 kJ/mol or above result in covalent bonds through chemisorption mechanism (Umoren et al., 2008). The value of ΔG_{ads} in H_2SO_4 reflects strong physical adsorption coupled with slight chemisorption mechanism. The negative values of ΔG_{ads} showed that the adsorption of BTU is spontaneous. The values of ΔG_{ads} calculated ranges between -30.23 and -31.63 kJ mol^{-1}. These values indicate the adsorption mechanism of BTU involves majorly physisorption through van der waals forces and partial chemisorption through the hydroxyl functional group. This is as a result of strong physical attraction between the BTU molecules and the steel surface forming a protective film that is covalently bond at the minimum.

3.9. Statistical analysis

The statistical analysis was evaluated for a confidence level of 95% i.e. a significance level of $\alpha = 0.05$. The ANOVA results (Fig. 12, Table 7) reveal that both experimental sources of variation (inhibitor concentration and exposure time) are statistically relevant and significant on the performance of BTU as reflected in the inhibition efficiency results with F-values of 528.12 and 116.64, both of which are greater than significance factor at $\alpha = 0.05$ (level of significance or probability). The statistical influence of the inhibitor concentration and exposure time are 79.2% and 15.2%. The inhibitor concentration and exposure time are significant model terms influencing inhibition efficiency of BTU on the corrosion behavior of the steel specimens. Both factors have strong influence on the performance of BTU i.e. the inhibition efficiency is directly proportional to the specific time of exposure and inhibitor concentration which must be taken into account for optimal performance outcome of BTU in the acid media, however greater emphasis must be placed on the inhibitor concentration with a statistical influence of 79.2%. On this basis the two independent variables significantly affects the inhibition efficiency of BTU in the acid media.

4. Conclusion

1. Experimental analysis of the corrosion inhibition properties of butan-1-ol showed the compound to be an efficient inhibitor in the acid environment with a maximum inhibition efficiency of 78.7% from weight-loss analysis and 80.9% from potentiodynamic polarization resistance technique at highest concentration of the alcohol.
2. Adsorption of butan-1-ol on the stainless steel aligns with Freundlich adsorption isotherm, proving that the relationship between the amount and concentration of BTU molecules absorbed onto the steel varies at different concentrations.
3. Thermodynamic variables of adsorption deduced reveal a physiochemical interaction with the steel surface and spontaneous adsorption of butan-1-ol.
4. Results from scanning electron microscopy analysis and X-ray diffractometry of the surface topography indicate the absence of compounds associated with accelerated corrosion reactions.
5. Statistical analysis with the use of ANOVA technique shows the strong influence of inhibitor concentration on the electrochemical performance of the compound.

Acknowledgement

The authors acknowledge the Department of Chemical, Metallurgical and Materials Engineering, Faculty of Engineering and the Built Environment, Tshwane University of Tech-

nology, Pretoria, South Africa for the provision of research facilities for this work.

References

Abbasov, V.M., Hany, M.A., Aliyeva, L.I., Qasimov, E.E., Ismayilov, I.T., Khalaf Mai, M., 2013. A study of the corrosion inhibition of mild steel C1018 in CO_2-saturated brine using some novel surfactants based on corn oil. Egypt. J. Pet. 22 (4), 451.

Amitha Rani, B.E., Bharathi Bai, J.B., 2011. Green inhibitors for corrosion protection of metals and alloys: an Overview. Int. J. Corros. http://dx.doi.org/10.1155/2012/380217.

Atkin, P.W., 1994. Physical Chemistry, fifth ed. Oxford University Press, Oxford, pp. 877.

Béla, L., Stainless steels and their properties. <www.outokumpu.com> (retrieved 03.04.14).

Chen, G., Zhao, J., 2012. Corrosion inhibition of imidazoline derivates with benzene rings on mild steel in CO_2-saturated brine solution. Chem. Res. Chin. Univ. 28 (4), 691.

Dieter, L., 2007. Corrosion and Surface Chemistry of Metals. EPFL Press, pp. 67.

Ebenso, E.E., 2003. Synergistic effect of halide ions on the corrosion inhibition of aluminium in H_2SO_4 using 2-acetylphenothiazine. Mater. Chem. Phys. 79, 58.

Giacomelli, F.C., Giacomelli, C., Amadori, M.F., Schmidt, V., Spinelli, A., 2004. Inhibitor effect of succinic acid on the corrosion resistance of mild steel: electrochemical, gravimetric and optical microscopic studies. Mater. Chem. Phys. 83, 124.

Hans, B., 2005. Corrosion in Concrete Structures. CRC Press, p. 193.

Hirozawa, S.T., 1995. Use of electrochemical noise in the study of corrosion inhibition of aluminium by gem diphosphonates. In: Proceeding of 8th European Symposium on Corrosion Inhibition, Ann University, Ferrara, Italy 1, 25.

Jianhai, Q., 2014. Stainless Steels and Alloys. <www.corrosionclinic.com> (retrieved 03.04.14).

Li, W.H., He, Q., Zhang, S.T., Pei, C.L., Hou, B.R., 2008. Some new triazole derivatives as inhibitors for mild steel corrosion in acidic medium. J. Appl. Electrochem. 38 (3), 289.

Maan, H., Shatha, A.S., Adeeb, H., Inas, M.A., 2012. Utilizing of sodium nitrite as inhibitor for protection of carbon steel in salt solution. Int. J. Electrochem. Sci. 7, 6941.

Mathiyarasu, J., Nehru, I.C., Subramanian, P., Palaniswamy, N., Rengaswamy, N.S., 2001. Synergistic interaction of indium and gallium in the activation of aluminium alloy in aqueous chloride solution. Anticorros. Met. Mater. 48 (5), 324.

Neha, P., Shruti, A., Pallav, S., 2013. Greener approach towards corrosion inhibition. Chin. J. Eng. http://dx.doi.org/10.1155/2013/784186.

Obi-Egbedi, N.O., Obot, I.B., 2013. Xanthione: a new and effective corrosion inhibitor for mild steel in sulphuric acid solution. Arab. J. Chem. 6 (2), 211.

Ochao, N., Moran, F., Pebre, N., 2004. The synergistic effect between phosphonocarboxylic acid salts and fatty amines for the corrosion protection of a carbon steel. J. Appl. Electrochem. 34, 487.

Oguzie, E.E., 2004. Influence of halide ions on the inhibitive effect of Congo red dye on the corrosion of mild steel in sulphuric acid solution. Mater. Chem. Phys. 87 (1), 212.

Physisorption, 2014. <http://en.wikipedia.org/wiki/Physisorption> (retrieved 03.04.14).

Quraishi, M.A., Sharma, H.K., 2002. 4-Amino-3-butyl-5-mercapto-1,2,4-triazole: a new corrosion inhibitor for mild steel in sulphuric acid. Mater. Chem. Phys. 78, 18.

Quraishi, M.A., Ansari, F.A., Jamal, D., 2004. Corrosion inhibition of tin by some amino acids in citric acid solution. Ind. J. Chem. Tech. 11 (2), 271.

Rudresh, H.B., Mayanna, S.M., 1977. Adsorption of n-decylamine on zinc from acidic chloride solution. J. Electrochem. Soc. 124 (3), 340.

Sastri, V.S., 2012. Green Corrosion Inhibitors: Theory and Practice. Wiley & Sons, pp. 141.

Satapathy, A.K., Gunasekaran, G., Sahoo, S.C., Amit, K., Rodrigues, P.V., 2009. Corrosion inhibition by Justicia gendarussa plant extract in hydrochloric acid solution. Corros. Sci. 51, 2848.

Shalaby, M.N., Osman, M.M., 2001. Synergistic inhibition of anionic and nonionic surfactants on corrosion of mild steel in acidic solution. Anti-Corr. Mets. Mats. 48 (5), 309.

Shylesha, B.S., Venkatesha, T.V., Praveen, B.M., Nataraja, S.E., 2012. Acid corrosion inhibition of steel by Lamotrigine. ISRN Corrosion. <http://dx.doi.org/10.5402/2012/932403>.

Terence, B., 2014. Austenitic Stainless. <www.metals.about.com> (retrieved 03.04.14).

Tsygankova, L.E., Esina, M.N., Vigdorovich, V.I., Shel, N.V., 2014. Study of steel corrosion inhibition in media containing H_2S and CO_2 by impedance spectroscopy and polarization resistance methods. Int. J. Corros. Scale Inhib. 3 (1), 48.

Umoren, S.A., Obot, I.B., Ebenso, E.E., 2008. Corrosion inhibition of aluminium using exudates gum from Pachylobus edulis in the presence of halide ions in HCl. E-J. Chem. 5 (2), 355.

Unuabonah, E.I., Olu-Owolabi, B.I., Adebowale, K.O., Ofomaja, A.E., 2007. Adsorption of lead and cadmium ions from aqueous solutions by tripolyphosphate-impregnated Kaolinite clay. Colloids Surf. A: Physicochem. Eng. Aspects 292, 202.

Winston, R.R., Papavinasam, S., 2000. Uhlig's Corrosion Handbook, second ed. John Wiley & Sons, Inc., pp. 1089–1096.

Xiumei, W., Ye, W., You, Z., Yaxin, G., 2012. Investigation of benzimidazole compound as a novel corrosion inhibitor for mild steel in hydrochloric acid solution. Int. J. Electrochem. Sci. 7, 2403.

Xiumei, W., Ye, W., Qing, W., Fangxiao, S., Zhaorong, F., Yanwen, C., 2013. Synergistic inhibition between bisbenzimidazole derivative and chloride ion on mild steel in 0.25 M H_2SO_4 solution. Int. J. Electrochem. Sci. 8, 2182.